Journal of Ethnopharmacology 261 (2020) 113042

Contents lists available at ScienceDirect

Journal of Ethnopharmacology

journal homepage: www.elsevier.com/locate/jethpharm

Croton urucurana Baillon stem bark ointment accelerates the closure of cutaneous wounds in knockout IL-10 mice

Thalia del Rosario Loyo Casao[a], Camila Graça Pinheiro[a], Mariáurea Matias Sarandy[b], Ana Caroline Zanatta[c], Wagner Vilegas[d], Rômulo Dias Novaes[e], Reggiani Vilela Gonçalves[b], João Paulo Viana Leite[a,*]

[a] Department of Biochemistry and Molecular Biology, Viçosa Federal University, 35570-900, Viçosa, Minas Gerais, Brazil
[b] Department of Animal Biology, Viçosa Federal University, 35570-900, Viçosa, Minas Gerais, Brazil
[c] Institute of Chemistry, São Paulo State University, Araraquara, 14800-900, São Paulo, Brazil
[d] Institute of Biosciences, São Paulo State University, 05508-900, São Vicente, São Paulo, Brazil
[e] Department of Structural Biology, Federal University of Alfenas, 37130-001, Alfenas, Minas Gerais, Brazil

ARTICLE INFO

Keywords:
Croton urucurana
Medicinal plant
Wound healing
Oxidative stress
Proanthocyanidins

ABSTRACT

Ethnopharmacological relevance: *Croton urucurana* Baill. (Euphorbiaceae) is a plant used in Brazilian popular medicine for the treatment of wound healing, inflammatory diseases, gastritis, infections, and hemorrhoids.
Aim: The present study aimed to evaluate the *in vivo* wound healing activity of an ointment based on ethanolic extract of *C. urucurana* stem bark, at concentrations of 5% and 10%, and to relate it with compounds that could be associated with this activity.
Materials and methods: Analyses by FIA-ESI-IT-MS^n were carried out to investigate the chemical composition of *C. urucurana*. Knockout IL-10 (n = 60) mice and wild type C57 (n = 12) mice were separated into 6 groups to evaluate the wound healing activity. Knockout IL-10 mice: SAL (0.9% saline); BAS (ointment base); SS (1% silver sulfadiazine); CR1 (ointment with extract of *C. urucurana* 5%); CR2 (ointment with extract of *C. urucurana* 10%); and wild mice C57: SALC57 (Saline 0.9%). A circular wound with 10 mm in diameter was generated on the dorsal of the animals. Tissue specimen of the wounds were removed on days 7 and 14 of the treatment for histopathological, oxidative status and analyses of pro-and anti-inflammatory cytokines in scar tissue.
Results: In the phytochemical profile, twelve proanthocyanidins were identified (in the form of monomers, dimers, trimers, and tetramers), based on (*epi*)catechin and (*epi*)gallocatechin. Furthermore, two quercetin derivatives and two alkaloids were detected. The groups treated with CR1 and CR2 ointments presented higher rate of wound closure, increased total number of cells, mast cells, blood vessels and higher deposition of type III and I collagen. In addition, they showed increased amount of pro-inflammatory cytokines (IL- 2 and IFN-γ), and anti-inflmatory cytokines (IL-4), on the 7th day of treatment.
Conclusion: The results presented support the popular use of preparations based on the bark of *C. urucurana* as a healing compound.

1. Introduction

Wound healing is a complex biological process involving different cell types, mainly keratinocytes, fibroblasts, endothelial cells and inflammatory cells. Moreover, it is characterized by an intense synthesis of extracellular matrix (Amorim et al., 2017). It can be divided into four stages: hemostasis, inflammation, proliferation and tissue remodeling (Fronza et al., 2014; Guo and DiPietro, 2010). In the first stage, the formation of the fibrin clot occurs to avoid tissue blood loss (Tang et al., 2014). Then, inflammatory cells are recruited to the lesion site attracted by proinflammatory cytokines that are continuously produced during this phase (Modarresi et al., 2019; Shapira et al., 2015).

In the proliferative phase, the synthesis of proinflammatory mediators persists, which results in the migration and proliferation of fibroblasts and endothelial cells, leading to granulation tissue formation, rich in cells and vessels (Abdulkhaleq et al., 2018; Valero et al., 2014).

* Corresponding author. Department of Biochemistry and Molecular Biology, Federal University of Viçosa, 35570-900, Viçosa, MG, Brazil.
E-mail addresses: thalia89.tlc@gmail.com (T.d.R.L. Casao), galpinheiro@gmail.com (C.G. Pinheiro), mariaureasarandy@gmail.com (M.M. Sarandy), anaczanatta@gmail.com (A.C. Zanatta), vilegasw@gmail.com (W. Vilegas), romuonovaes@yahoo.com.br (R.D. Novaes), reggysvilela@yahoo.com.br (R.V. Gonçalves), jpvleite@ufv.br (J.P. Viana Leite).

https://doi.org/10.1016/j.jep.2020.113042
Received 12 June 2019; Received in revised form 25 March 2020; Accepted 28 May 2020
Available online 10 June 2020
0378-8741/

Angiogenesis, which characterizes this phase, is stimulated by some mediators, including the tumor necrosis factor alpha (TNF-α), which promotes endothelial cell proliferation and neoangiogenesis (Samy et al., 2014). In this phase, it is also observed the synthesis of anti-inflammatory mediators, such as IL-10, that control the inflammatory process and prevent its chronification (Modarresi et al., 2019; Oliveira et al., 2011). In the last phase of the process, known as remodeling, type III collagen is replaced by type I collagen, which is stronger and resistant to traction. This leads to tissue maturation and scar formation that resembles healthy skin (Valero et al., 2014).

Interleukin 10 (IL-10) is an anti-inflammatory cytokine and controls the signaling in macrophages and neutrophils and is necessary to prevent abnormal regulation of responses to the normal inflammatory. In addition, regulates angiogenesis by inducing the cell-type dependent expression of both angiogenic and angiostatic factors. Thus, IL-10 knockout mice are a desirable animal model, once may develop greater inflammation and presented reduced vascularization during the healing process. Currently, is known that effective tissue repair occurs by balance of anti and proinflammatory mediators and proper vascularization. Prolonged inflammation can result in detrimental tissue injury and reduced number of blood vessels can slow down the healing process (Eming et al., 2007; Khezri et al., 2019). So, how our objective was study the effect of the new therapeutic formulation obtained from *C. urucurana* for treatment of cutaneous healing, we believed that this animal model is very valid, because it allows us to study this pathology condition in the extreme conditions, with low vascularization and high profile inflammatory. Thus, the use of this animal model enhances the inflammatory process and allows us to have a better understanding of the action of the herbal medicine tested in the skin repair process.

In Brazilian traditional medicine, medicinal preparations made from the stem bark of *Croton urucurana* Baillon, family Euphorbiaceae, is used for wound healing. Popularly known as "dragon's blood", "water bleed", "urucurana" and "lucurana", this plant is used for different purposes, such as wound healing, anti-hemorrhagic, anti-inflammatory, antiseptic and antiviral treatments (Gupta et al., 2008; Rieder et al., 2011). Secondary metabolites of the diterpenes, alkaloids, flavonoids and tannins classes have already been identified in *C. urucurana* (Cordeiro et al., 2016). Bark methanol extract showed gastroprotective activity in experimental models in rats, without causing toxicity, increasing mucus production and reducing gastric acidity, which demonstrated its *in vivo* anti-inflammatory and analgesic effect (Wolff et al., 2012). On the other hand, how the ointments are considered a simplest formulation and easy to handle and apply, leading to a high preference for this type of medication and presented good results to healing activity when compared to gel (Patil et al., 2012). We aimed to evaluate the topical action of ointment based on ethanolic extract of *C. urucurana* bark in the process of cutaneous repair in Knockout mice for IL-10In addition, it also aims to determine the phytochemical profile of the extract to demonstrate that the compounds associated with the healing activity of the plant may be used as the future active markers for the standardization of herbal medicines.

2. Material and method

2.1. Plant material

The plant material (*C. urucurana* stem barks) was collected in the city of Rosário da Limeira, Minas Gerais, Brazil, at the coordinates 20°33' - 21°00′S and 42°40' - 40°20′W, where the Atlantic Forest biome predominates. An herbarium voucher specimen was herborized and deposited in the Herbarium VIC, at the Viçosa Federal University de (number VIC 47.928).

2.2. Extract preparation

The stem barks were dried in a ventilated oven at 40 °C. The extract was prepared from the dried and comminuted hulls (1.5 kg), and subjected to exhaustive maceration with 95% ethanol (v/v). Subsequently, the extract was concentrated on a rotary evaporator until the complete removal of the solvent so as to obtain the *C. urucurana* extract. The extract obtained (96.58g) was stored under refrigeration in an amber glass bottle. The w/w extraction yield for the stem bark extract based on dry plant material was 6.44%.

2.3. Chemical analysis by FIA-ESI-IT-MS/MSn

The chemical profile of *C. urucurana* extract was obtained by direct flow infusion analysis (FIA), using a syringe pump with a flow rate of 5 μL/min, in mass spectrometer with ionization source by electrospray (ESI), in positive and negative modes (Thermo, San Jose, EUA) equipped with analyzer *ion trap (*IT) linear (Thermo Scientific LTQ XL) and the Xcalibur software system. The capillary tension was −35 V; the spraying voltage, 5 kV; and the tube lens, −100 v. The capillary temperature was 280 °C. Nitrogen was used as nebulizer and carrier gas for flow. The complete scanning analysis was recorded in the *m/z* 100–1500. The multi-stage fragmentation (ESI-MS^n) was performed using the collision-induced dissociation (CID) method against helium gas for ion activation. Two events were performed during the mass spectrometer analysis. First, the full scan mass spectrum (*full-scan*), in order to acquire the data of ionized compounds within the established range *m/z* 200–1500. In the second event, the MS/MS experiment was performed with 30% collision energy and activation time of 30 ms., using scan dependent data from the full scan. The collision energy for MS/MS was adjusted in 30–40 eV. Successive fragmentations were obtained for the ion products achieved (Tala et al., 2013). Mass spectra were processed in Xcalibur software (version 2.0). The annotation of the compounds using untargeted mass spectrometry analysis was performed based on MSn fragmentation patterns (literature data) and through spectral similarity to reference databases, such as METLIN (Smith et al., 2005), MassBank (Horai et al., 2010) and KNApSAcK Core System (Afendi et al., 2012).

2.3.1. Clean up by SPE

The preparation of the extract consisted of one clean up step by extraction in solid phase with the use of cartridges of RP18. The cartridges were previously activated with methanol (4 mL) and equilibrated with methanol/ultrapure water (85:15, v/v) (4 mL). The extracts (10 mg) to be applied in the SPE support were previously solubilized in 1.5 mL of the methanol/water solution (90:10, v/v), eluted with the same proportion of mobile phase and thereafter dried in compressed air. After drying, 2 mg of each extract was resuspended in 2 mL of methanol/water (90:10, v/v), which provided a solution with a concentration of 1 mg.mL-1. Finally, solutions were filtered on a Millex® PTFE filter with pore size of 0,22 μm.

2.4. Preparation of ointment

Two formulations of different concentrations were prepared with 5% and 10% of extract of the *C. urucurana*, employing for both a base (hydrophilic) ointment composed of a mixture of polyethylene glycol (Macrogol) and propylene glycol.

2.5. In vivo healing assay

2.5.1. Animals

Knockout mice for IL-10 and wild-type female C57 mice, with mean weight of 15 ± 2 g, at 8 weeks of age, from the Laboratory of Experimental Pathology, were randomly allocated into groups at the Animal Nutrition Laboratory of the Federal University of Viçosa. The animals were kept in individual cages with cycles of 12 h of clarity and 12 h of darkness and controlled temperature (22 ± 2 °C, 60–70% humidity). The animals had access to water and commercial feed *ad*

libitum. All procedures were approved by the Animal Ethics Committee for the Use of Animals in research, adopted by the Viçosa Federal University (protocol nº 41/2017).

2.5.2. Experimental design

Wild C57 mice (n = 12) were used as controls for the knockout as the SALC57 group: wounds treated with saline solution 0.9% (negative control). Knockout animals for IL-10 (n = 60) were randomly distributed in 5 groups (n = 12): SAL: wounds treated with 0.9% saline solution (negative control); BAS: wounds treated with topical base of the ointment composed of polyethylene glycol (Macrogol 400 and 4000) and propylene glycol; SS: wounds treated with 1% Silver Sulfadiazine® ointment (positive control); CR1: wounds treated with topical ointment of *C. urucurana* bark ointment 5%; CR2: wounds treated with topical ointment of the ointment of *C. urucurana* 10%. After the surgical procedure, the wounds were cleaned with saline solution (0.9%) and treated with topical application of the SAL, BAS, SS, CR1 and CR2 ointments. The choice of dose was based on a phytotherapic Fitoscar® (*Stryphnodendron adstringens* bark extract - 30% of total phenols and 27 mg/g of total tannins; Brazilian ANVISA/Ministry of Health registration No. 1.0118.0605) that has the phytochemical composition similar to the composition of *C. urucurana*. All treatments were initiated 12 h after wounding for the 14 days of the experiment.

2.5.3. Realization of surgical excision wounds

The animals were anesthetized with pentobarbital (70 mg/kg body weight), depilated in the dorsolateral region and the lesion area was degreased with ether (Merck, Rio de Janeiro, Brazil). Then, ethanol (70%) and iodopovidone (10%) were applied for asepsis (Johnson Diversey®, Rio de Janeiro, Brazil). A 10 mm diameter circular excision wound was made by surgical incision in the skin and subcutaneous tissue with a scalpel until the dorsal muscular fascia was exposed (Sarandy et al., 2018). On day 0, the tissue was removed uninjured and the treatment started. On the 7th day of treatment, the tissue samples of half of the animals of each group (n = 6) were collected. Next, these animals were euthanized by cardiac puncture exsanguination following general anesthesia with pentobarbital (210 mg/kg body weight). After 14 days of treatment, scar tissue was removed from the remaining animals (n = 6). The fragments of the skin removed were separated into three portions for histological, oxidative and immunological analysis.

2.5.4. Area and rate of wound contraction

The area and index of wound contraction were evaluated after the 7th and 14th days, using 320 × 240 pixel scanned images (24 bits/pixel) obtained by a digital camera (Sony W320, Tokyo, Japan). The wound area was calculated by planimetry, using the Image-Pro Plus 4.5® software system (Media Cybernetcs, Silver Spring, USA). The wound contraction rate (WCI) was calculated using the following equation: initial wound area (Ao) - area measured on a given day (Ai)/ initial wound area (Ao) x 100 (Gonçalves et al., 2016).

2.5.5. Histopathological analysis

The fragments were fixed in Karnovsky's solution for 24 h, dehydrated in ethanol, diaphanized in xylol and embedded in paraffin. Next, 4 μm-thick histological sections, obtained on a rotating microtome, were mounted on histological slides. One in ten cuts was used to avoid repeated analysis of tissue constituents. The sections were stained with Hematoxylin and Eosin (H&E) for analysis of fibroblasts and blood vessels (Sarandy et al., 2017) by the Sirius Red technique for analysis of collagen fibers under polarization microscopy (Rosa et al., 2018) (Sigma, St. Louis, Mo, USA). The thick collagen fibers (type I) appeared in bright shades ranging from red to yellow, while the fine reticular fibers (type III collagen) were bright green (Novaes et al., 2015). Resorcin fuchsin was used to mark elastic fibers (Rosa et al., 2018).

The visualization of the slides and capture of the images were performed using the BX-60® light microscope (Olympus, Tokyo, Japan) connected to a digital camera (Olympus, São Paulo, Brazil). A total area of 1.53×10^6 μm^2 was submitted to stereological analysis. Ten histological fields were randomly sampled in each section of the skin using a 20× objective lens. A grid of 300 dots was projected onto each image. Volumetric density (Vv) parameters were calculated by counting the points on fibroblasts, blood vessels and type I and type III collagen, using the following ratio: Vv = (PP/PT) × 100, where PP is the number of points occurring over the structure of interest and PT is the total number of points in the test system (Sarandy et al., 2015).

Sections of scar tissue stained with toluidine blue were used for the identification of mast cells. Using a 40× objective lens, 10 histological fields per slide were randomly analyzed, totaling an area of 6.21×10^6 μm^2. The number of mast cells per unit area was calculated according to the ratio QA = Σ mast cells/AT, where Σ is the sum of mast cells within an area and AT (total area) = πr^2 (Leclere et al., 2006).

2.5.6. Biochemical analysis

Tissue samples removed from each wound were immediately frozen in liquid nitrogen (−196 °C) and stored in a freezer at −80 °C. These samples were homogenized in phosphate buffer and centrifuged at 4 °C. The levels of the antioxidant enzyme activities were analyzed on the supernatant as superoxide dismutase (SOD) decomposition rate, following Siddiqui et al. (2005) protocol, and catalase (CAT) measured by the hydrogen peroxide (H_2O_2) consumption (Salvi et al., 2007). GST was measured by the formation of glutathione-2,4-dinitrobenzene torque and estimated by the change in absorbance at 340 nm, for 60s, and the results were expressed as $\mu mol.min^{-1}.g^{-1}$ (Habig et al., 1976). The total protein was determined by the Lowry et al. (1951) method, using bovine serum albumin as standard and the data were normalized according to the total protein levels in the supernatant.

2.5.7. Cytokine expression analysis

Scar tissue samples, collected on days seven and 14, were frozen at −80 °C, homogenized in PBS 7.4 buffer containing 0.05% Tween and centrifuged at 3500g, for 30 min. The supernatant was analyzed with the use of immunoassay kits, by the BD Cytometric Bead Array (CBA)/ Mouse Th1/Th2/Th17 of the segment of BD cytometry notes (CBA) (BD Biosciences, San Diego, CA, EUA). The data were collected using FACSCalibur and analyzed with the use of the FCAP 3.0 software system (BD Biosciences, San Diego, CA, EUA). The dosages of the cytokine IL-2 (interleukin-2), IL-4 (interleukin-4), IL-6 (Interleukin-6), IL-10 (Interleukin-10), IFN-γ (Interferon-γ), IL-17 (Interleukin-17) were provided for flow cytometry, following the manufacturer recommendations.

2.5.8. Statistical analysis

The data were reported as mean and standard deviation (mean ± SD). The comparisons between the groups with parametric distribution (Kruskal-Wallis) were performed using unidirectional Anova. For non-parametric data, kruskal-wallis was performed. Statistical significance was defined as $p < 0.05$. The analyses were performed using GraphPad Prism 5.0® (GraphPad Software Inc., SanDiego, California, USA).

3. Results and discussion

3.1. Phytochemical profile

Compounds derived from proanthocyanidins were identified by FIA-ESI-IT-MS^n, in the negative mode. Proanthocyanidins comprise an extensive group of polyphenolic compounds, also known as condensed tannins, which are mainly formed by oligomers based on (*epi*)catechin or (*epi*)gallocatechin (Lv et al., 2015). For the analysis of the proanthocyanidins present in *C. urucurana,* the negative mode ionization was more sensitive and selective than in the positive mode, probably due to the acidic character of the phenolic groups. The therapeutic potential of

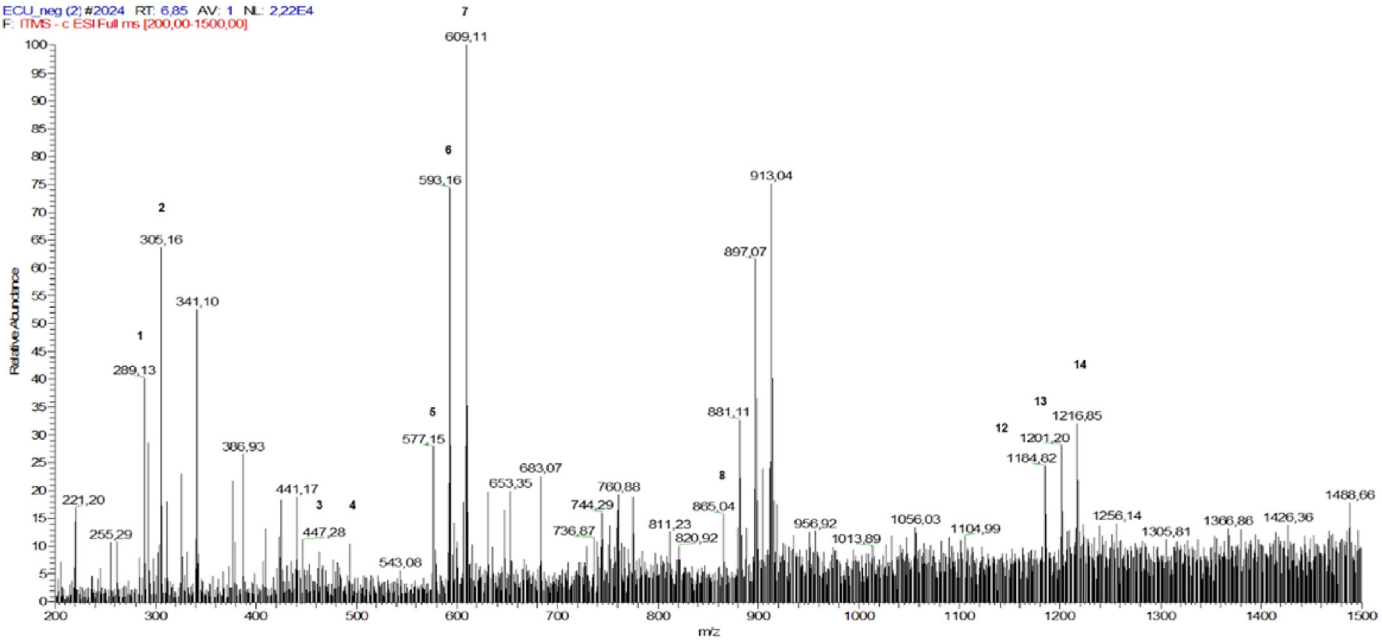

Fig. 1. Direct infusion ESI-MS spectrum of *C. urucurana* extract in the negative mode.

Table 1
Identification of compounds in C. urucurana extract by $[M-H]^-$ ion, MS^n fragments using FIA-ESI-IT-MS.^{n}.

N	$[M-H]^-$	MS^n	Compound
1	289	271, 245, 203, 175	(*epi*)catechin
2	305	287, 261, 221, 203,179	(*epi*)gallocatechin
3	447	429, 301, 179	quercetin-O-rhamnoside
4	493	461, 443, 331, 169	methoxiquercetin-*O*-glucoside
5	577	559, 451, 425, 407, 289	(*epi*)catechin-(*epi*)catechin
6	593	575, 425, 423, 407, 289	(*epi*)gallocatechin-(*epi*)catechin or (*epi*)catechin-(*epi*)gallocatechin
7	609	441, 423, 305	(*epi*)gallocatechin-(*epi*)gallocatechin
8	865	713	(*epi*)catechin-(*epi*)catechin-(*epi*)catechin
9	881	863, 755, 695, 593, 467	(*epi*)catechin-(*epi*)catechin-(*epi*)gallocatechin
10	897	729, 711, 693, 593, 559	(*epi*)gallocatechin-(*epi*)gallocatechin-(*epi*)catechin
11	913	865, 787, 755, 727, 607	(*epi*)gallocatechin-(*epi*)gallocatechin-(*epi*)gallocatechin
12	1185	1059, 999, 813	(*epi*)catechin-(*epi*)catechin-(*epi*) gallocatechin-(*epi*)gallocatechin
13	1201	1075, 1015	catechin-(*epi*)gallocatechin-(*epi*)gallocatechin–(*epi*)gallocatechin
14	1217	1091, 1031	(*epi*)gallocatechin-(*epi*)gallocatechin -(*epi*)gallocatechin- (*epi*)gallocatechin

proanthocyanidins demonstrated by (Hemmati et al., 2014; Schmidt et al., 2011; Tatsuno et al., 2012; Wen-Guang et al., 2001) relate the import of this compound in wound healing. Fig. 1 shows the mass spectrum in full scan indicating ions $[M-H]^-$ referring to the secondary metabolites present in *C. urucurana*. MS/MS fragmentation pattern for the identified compounds from FIA-ESI-IT-MS/MSn is described in Table 1 and supplementary material.

In the FIA-ESI-IT-MS^n spectrum, in the positive mode, the protonated quasi-molecular ions at *m/z* 342 $[M+H]+$and at *m/z* 344 $[M+H]+$indicated the presence of two alkaloids previously reported for *C. urucurana* (Cordeiro et al., 2016). The analysis of these protonated ions with their respective product ions at *m/z* 297, 282, 265 and 237 generated from the fragmentation of *m/z* 342 $[M+H]^+$ and the product ions (?) *m/z* 299 and 253 from the precursor ion *m/z* 344 $[M+H]^+$ were consistent with the literature data reported for the compounds magnoflorin and tembetarin (Yan et al., 2013). For both alkaloids, the fragmentation pattern favored the formation of the base peak with the loss of a very characteristic C_2H_7N unit. The initial loss of the amine group and successive losses of the substituent groups are well established for ESI fragmentation of aporphic alkaloids (Silva et al., 2012).

3.2. Wound area and wound contraction index

The wound area and contraction rate were evaluated on days 7 and 14. The wound area was significantly reduced in the groups treated with CR1 and CR2, when compared to groups SALC57, SAL and BAS, on days 7 and 14 ($p < 0.05$) (Table 2 and Fig. 2). Regarding the rate of wound contraction, the CR1 and CR2 groups presented a higher rate of lesion closure when compared to the SALC57, SAL, and BAS groups on days 7 and 14. A high rate of wound closure and the decreased wound areas in the groups treated with CR1 and CR2 may be related to the presence of the flavonoids and proanthocyanidins found in this extract. Sarandy et al. (2017) have shown that the *Strychnos pseudoquina* extract enriched with phenolic compounds, including quercetin flavonoid, has high healing capacity, since it stimulates the rapid closure of the wound and promotes matrix synthesis, besides stimulating cell and vascular proliferation in cutaneous wounds of rats. Similarly, Lopes et al. (2013) applied an ointment with proanthocyanidin-enriched extract of *Croton lechleri* under rat cutaneous wounds at concentrations of 0.1 μg/mL to 1 μg/mL and observed that the wound area decreased and a thick tissue was formed on day 7 of the treatment. In addition, Machado et al. (2015) showed that the ethanolic extract of *C. urucurana* shells, when applied topically to mice, stimulated the wound closure rate after 12 days. It indicates that this action is probably related to the high level of

Table 2
Area (mm^2) and wound contraction index (WCI) (%) in wild C57 mice and IL-10 knockout mice treated with ointment based on C. urucurana extract.

Day	Área/WCI	SALC57	SAL	BAS	SS	CR1	CR2
0	Área (mm^2)	86.87 ± 11.44	88.01 ± 15.18	90.04 ± 7.96	85.09 ± 8.51	87.61 ± 12.26	80.00 ± 4.97
	WCI (%)	0.00 ± 0.00	0.00 ± 0.00	0.00 ± 0.00	0.00 ± 0.00	0.00 ± 0.00	0.00 ± 0.00
7	Área (mm^2)	57.03 ± 9.23	58.25 ± 7.31	58.17 ± 5.60	47.18 ± 2.89	23.95 ± 4.72*	24.21 ± 6.68*
	WCI (%)	31.26 ± 17.31	34.66 ± 15.90	34.03 ± 4.59	44.84 ± 9.32	73.83 ± 1.96*	72.71 ± 6.78*
14	Área (mm^2)	3.17 ± 0.70	3.58 ± 0.76	3.18 ± 1.06	2.81 ± 0.97	0.96 ± 0.28*	0.89 ± 0.24*
	WCI (%)	96.70 ± 0.46	96.54 ± 0.44	96.38 ± 0.46	97.42 ± 0.46	98.84 ± 0.34*	98.86 ± 0.31*

proanthocyanidins and other phenolic compounds in the extract of this plant (Salatino et al., 2007).

Area (mm^2) and wound contraction index (WCI) in wild C57 mice and IL-10 knockout mice on days 0, 7 and 14. SalC57: wild group C57, 0.9% saline solution. IL-10 knockout groups: SAL, 0.9% saline; BAS, ointment base; SS, 1% silver sulfadiazine; CR1, ointment of *C. urucurana* 5%; CR2, ointment of *C. urucurana* 10%. The data are represented as mean ± SD, $P < 0.05$ (Kruskal-Wallis test). ∗Statistically different compared to SALC57, SAL and BAS.

3.3. Histopathological analysis

The animals treated with CR1 and CR2 presented a higher number of cells on days 7 and 14 when compared to SALC57, SAL, and BAS. The positive control group treated with 1% silver sulfadiazine (SS) presented increased cellularity on day 14 when compared to SALC57 and SAL, but lower values than CR1 and CR2 (Fig. 3A). This cell proliferation potential was reported in a review by Gupta et al. (2008), on the effect of the extract of *C. urucurana* on cell culture of fibroblasts. The results showed an increased number of these cells after the application of the extract, which corroborates our findings regarding vascular proliferation, since the groups treated with *C. urucurana* presented an increased number of vessels in the cicatricial tissue. It is clear that the cells require nutrients and oxygen to proliferate adequately, and this supply only occurs in well vascularized tissues (Kant et al., 2015; Samy et al., 2014). Our results showed that the groups that received CR1 and CR2 and SS presented an increased number of vessels on day 7, when compared to the other groups, especially the group that received the lowest concentration (CR1). On day 14, the CR1 and CR2 groups presented increased vascularization when compared to all the other groups ($p < 0.05$) (Fig. 3B). It is known that 1% silver sulfadiazine is a drug commonly used to treat wounds due to its high antimicrobial and anti-inflammatory power (Ferreira and Paula, 2013; Fisher et al., 2003; Ragonha et al., 2005). We observed that *C. urucurana* ointment was more effective in promoting cell and vascular proliferation in cutaneous scar tissue than 1% silver sulfadiazine ointment (Fig. 3A and B and Supplementary Fig. 1). This indicates the high capacity of the *C. urucurana* extract to promote the recovery of the injured tissues and consequently accelerate their closure.

In relation to the number of mast cells in the tissue, on days 7 and 14, the highest concentration of these cells was observed in the CR1 and CR2 groups. On day 14, the CR2 group presented the highest concentration of these cells ($p < 0.05$) (Fig. 3C and Supplementary Fig. 1). Studies have shown that mast cells are important in the regulation of the metabolism of other cells, favoring tissue angiogenesis by releasing a series of mediators, such as Vascular Endothelial Growth Factor (VEGF), Fibroblast Growth Factor-β (FGF-β) (TGF-β), tumor necrosis factor α (TNF-α) and interleukin-8 (IL-8) (Farahpour et al., 2015; Johnson and Wilgus, 2014; Krystel-Whittemore et al., 2016). Similar results were found by Sarandy et al. (2018), in their analysis of the healing effect of *Strychnos pseudoquina* in healthy and diabetic animals. It is interesting to observe that, similarly to *C. urucurana*, the *S. pseudoquina* extract enriched with phenolic compounds acted in the inflammatory phase of the repair process by stimulating cell proliferation, especially increasing the mast cells in the tissue. It is noteworthy that the inflammatory process in the early phase of tissue recovery is necessary for the proliferative and remodeling phases to occur adequately and satisfactorily (Gonzalez et al., 2016; Landén et al., 2016; Manzuoerh et al., 2019). Furthermore, it should be considered that the animals used in this study are knockout for IL-10, a potent anti-inflammatory cytokine, and that these animals usually present a more pronounced inflammatory process (Jara et al., 2018). However, in this

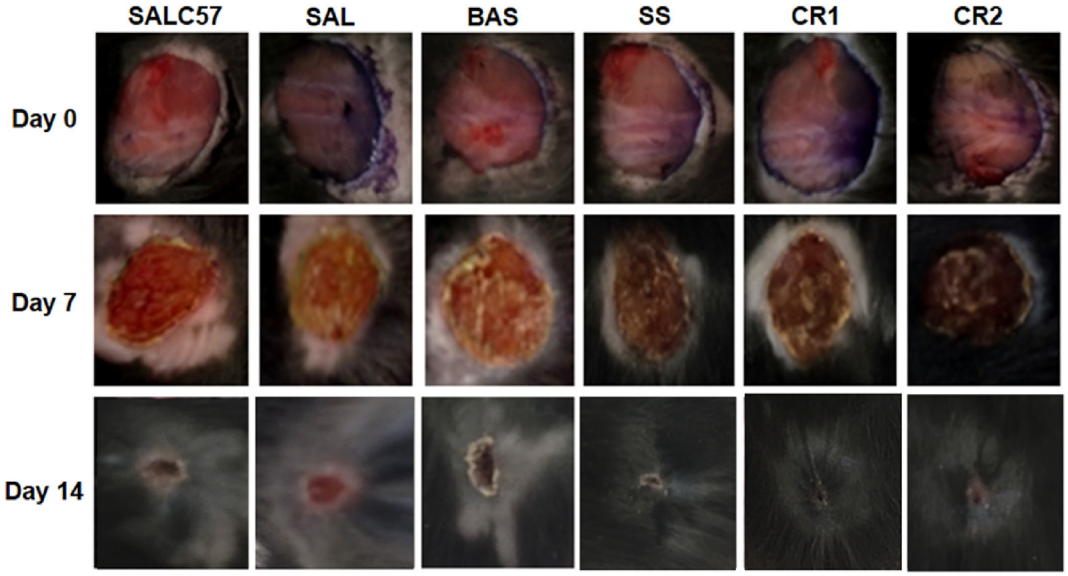

Fig. 2. Photographs representative of wild-type C57 mice (SALC57) and IL-10 knockout mice injured on days 0, 7 and 14 were expressed in 5 groups: SAL: saline 0.9% w/v. BAS: ointment base; SS: 1% silver sulfadiazine; CR1: ointment of *C. urucurana* 5% w/w; CR2: ointment of *C. urucurana* 10% w/w.

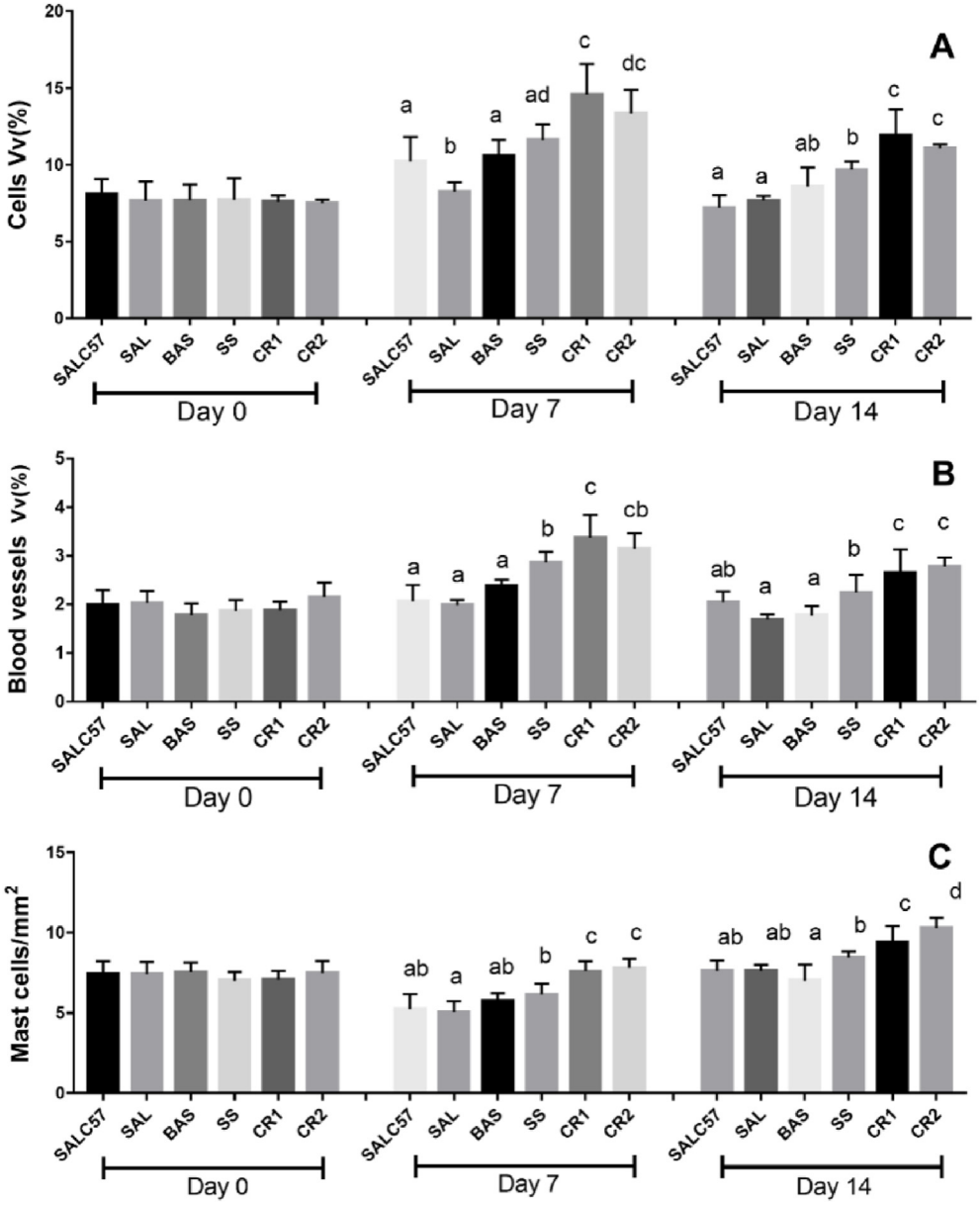

Fig. 3. A - Total number of cells, B - blood vessels and C - mast cells in the scar tissue of wild C57 mice and IL-10 knockout mice on days 0, 7 and 14. SALC57: wild group C57, saline solution 0.9%. IL-10 knockout groups: SAL, 0.9% saline; BAS, Ointment Base; SS, 1% silver sulfadiazine; CR1, ointment of *C. urucurana* 5%; CR2, ointment of *C. urucurana* 10%. Data are represented as mean ± SD. Different letters indicate significant differences between groups $p < 0.05$ (Kruskal-Wallis test).

study, this genetic change was not sufficient to promote chronic inflammation during cutaneous repair nor delay the healing process of wounds. We believe that these results are due to the proanthocyanidins present in the *C. urucurana* extract. These compounds are known for their anti-inflammatory and antimicrobicidal effect that may accelerate the wound healing process (Salinas-Sánchez et al., 2017; Tatsuno et al., 2012; Wen-Guang et al., 2001). In addition, although there is evidence that immune mediators may interact with different molecules in the treatment of diseases involving inflammation (Venkatesha et al., 2011) in this study, control groups (SALC57, SAL, BAS and SS) were used comparatively, with objective of exclusion of any interference of the extract with IL-10.

In our study, when the components of the matrix were analyzed, a predominance of type I collagen was observed on days 7 and 14 in the SS, CR1 and CR2 groups, mainly in the CR1 group ($p < 0.05$) (Fig. 4A). The predominance of type III collagen fibers was observed in the CR1 and CR2 groups, on days 7 and 14, compared to the other groups ($p < 0.05$) (Fig. 4B). It is known that in the early stages of the cicatricial process, the formation of granulation tissue rich in cells, vessels and collagen III, fragile and weak, is essential for the occurrence of the remodeling phase (Thandavarayan et al., 2015). As the process evolves, the type III collagen fibers are replaced by type I collagen, which is stronger and presents cross-links between its fibrils, which gives the tissue tensile strength (Muthusubramaniam et al., 2014). Thus, the granulation tissue should be progressively replaced by a tissue that resembles the original skin to promote a harmonious healing process. These changes are striking features of the healing remodeling phase, when the final scar formation occurs (Kant et al., 2015). Similar results were found by Amorim (2017), who observed that the application of the extract of *Copaifera paupera* in skin lesions accelerates the deposition of type I collagen, probably due to the predominance of flavonoids, such as quercetin, which accelerate the synthesis of collagen by fibroblasts. Similarly, Ganeshkumar et al. (2012), analyzed the extract from *Acalypha indica* (Euphorbiaceae) and observed increased

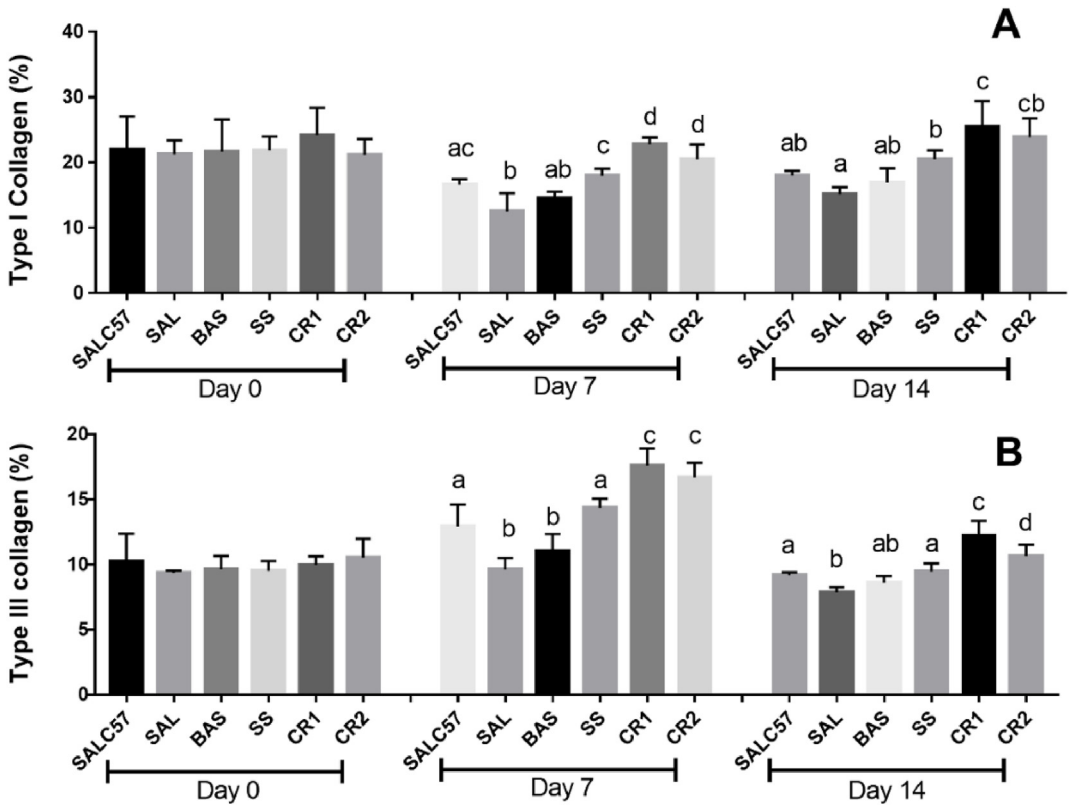

Fig. 4. A - Proportion of collagen fibers of type I and B - Proportion of collagen fibers of type I III in the scar tissue of wild C57 mice and IL-10 knockout mice on days 0, 7 and 14. SALC57: wild group C57, saline solution 0.9%. IL-10 knockout groups: SAL, 0.9% saline; BAS, Ointment Base; SS, 1% silver sulfadiazine; CR1, ointment of *C. urucurana* 5%; CR2, ointment of *C. urucurana* 10%. Data are represented as mean ± SD. Different letters indicate significant differences between groups $p < 0.05$ (Kruskal-Wallis test).

collagen production. Studies demonstrate that topical application of herbal extracts or phytochemicals dramatically enhances epidermal permeability and modifies the barrier function of the skin in animal studies (Hou et al., 2013, 2012; Man et al., 2011). In addition, a variety of herbal compounds such as polyphenols and flavonoids act on membrane lipids and change cell membrane properties affecting epidermal permeability (Beecher, 2004; Tsuchiya, 2015). Although it the fragment skin was surgically removed and the ointment with the extract was applied directly over the lesions, facilitating the permeability of the extract, the subsequent phase (day 7), there was present of granulation tissue, which is mainly made up of type III collagen, glycosaminoglycans and proteoglycans, forming an extremely thin tissue that also directly received the ointment containing the extract (Shedoeva et al., 2019). The extremely thin thickness of the granulation tissue suggest that there was good permeability of the *C. urucurana* extract (7 days).

This effect may be associated with the abundant concentration of phenolic compounds, flavonoids and tannins found in this extract. The application of compounds rich in tannins is known for stimulating the synthesis of collagen fibrils and increasing the interaction among them through the formation of cross-bridges between collagen microfibrils, which gives strength and resistance to the tissue (Thakur et al., 2011).

3.4. Biochemical analysis

On day 7, the analysis of the antioxidant profile showed increased of the enzyme superoxide dismutase (SOD) in the SS, CR1 and CR2 groups ($p < 0.05$), when compared to the others (Fig. 5A). On day 14, the highest concentration of this enzyme was observed in the SAL, SS and CR1 groups ($p < 0.05$). On day 7, catalase enzyme showed increased concentration in the CR1 and CR2 groups; and on day 14, the SS, CR1, and CR2 groups presented higher CAT concentration when compared to the other groups ($p < 0.05$) (Fig. 5B). In relation to glutathione S-transferase (GST), on day 7, the SS and CR1 treated groups presented higher concentration of this enzyme when compared to the other groups ($p < 0.05$) (Fig. 5C). On day 14, the group treated with CR1 presented higher values of GST when compared to the other groups ($p < 0.05$).

These enzymes are extremely important in the fight against the generation of free radicals within the cell (Fujiwara et al., 2016). When a tissue is damaged, the generation of reactive oxygen species (ROS) usually increases, which changes the lipids, proteins, and DNA of the cell, thus causing tissue stress and decreased cellular function (Guo and DiPietro, 2010). The formation of these radical species is controlled by antioxidant enzymes. Therefore, during the skin repair process, the amount of these enzymes should desirably be increased to protect the tissue from the activity of these radicals (Limón-Pacheco and Gonsebatt, 2009). SOD and CAT are the first line of defense by neutralizing superoxide (O*) and hydrogen peroxide (H_2O_2), respectively, which are produced during the transport of electrons through the mitochondrial transport chain during ATP formation (Fujiwara et al., 2016). In a later step, we can highlight the action of GST, which eliminates the free radicals generated in the final phase of the oxidative process that were not neutralized by the other two enzymes (Antunes-Neto et al., 2006). We believe that the increase in the antioxidant system stimulated by CR1 and CR2 was extremely important to accelerate the recovery of the damaged cutaneous tissue, since we can associate the increase of these enzymes with decreased free radical levels and consequent reduced inflammatory response and accelerated wound healing. It is important to highlight the difference between the treatments with the ointments and that the best results were found at the lowest dose (CR1). The antioxidant action of *C. urucurana* extract is due to the high presence of phenolic compounds, such as

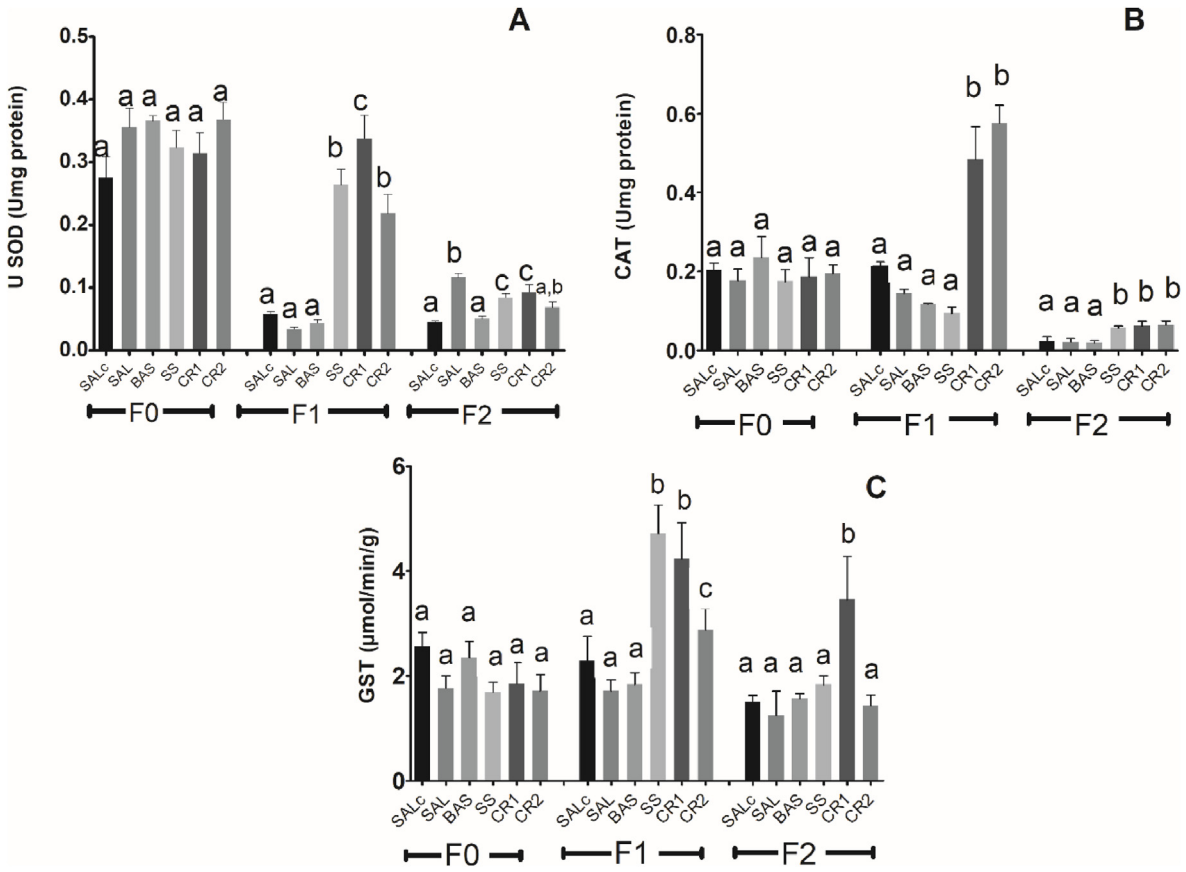

Fig. 5. Levels of antioxidant enzymes: A-Superoxide dismutase (SOD), B-Catalase (CAT) and C-Glutathione S-transferase (GST) in the cicatricial tissue of wild C57 mice and IL-10 knockout mice on days 0, 7 and 14. SALC57: wild type C57 group, 0.9% saline solution. IL-10 knockout groups: SAL, 0.9% saline; BAS, Ointment Base; SS, 1% silver sulfadiazine; CR1, ointment of *C. urucurana* 5%; CR2, ointment of *C. urucurana* 10%. Data are represented as mean ± SD. Different letters indicate significant differences between groups $p < 0.05$ (Kruskal-Wallis test).

proanthocyanidins, which are known for their antibacterial, anti-inflammatory and healing properties (Hemmati et al., 2014; Schmidt et al., 2011). These compounds have high ability to capture free radicals and chelate transition metals, such as iron and copper, which prevents them from catalyzing peroxidation chain reactions (Morry et al., 2017; Roleira et al., 2015).

3.5. Analysis of pro-and anti-inflammatory cytokines in scar tissue

Regarding the inflammatory profile, we observed that the proinflammatory cytokines (IL-2 and INF-γ) were increased in the CR1 and CR2 groups at day 7 when compared to the other groups (Fig. 6A and B). On the 14th day, the groups CR1 and CR2 presented low values for these markers, but the SS treated group presented increased values for INF-γ and IL-17 ($p < 0.05$). However, there was no difference between wild (C57) animals and knouckout animals that received only saline (Fig. 6A, B and C).

When we analyzed anti-inflammatory markers, we observed that animals receiving CR1 and CR2 presented high levels of IL-4 and all knockout animals presented low values for IL-10, except the SALC57 group, which normally expresses cytokine ($p < 0.05$). However, there was no difference between wild (C57) animals and knouckout animals that received only saline (Fig. 7A and B).

Our results reveal that there is no difference between wild (C57) and knockout animals for pro and anti-inflammatory cytokines, except for IL-10. Considering that IL-10 is an anti-inflammatory cytokine of T regulatory profile, its depletion could potentiate the inflammatory process and impair the healing progress (Hsu et al., 2015; Khezri et al., 2019; Modarresi et al., 2019). However, the effect of this cytokine on the healing process is not completely understood yet. There is evidence that depletion of specific cytokines may generate a counter regulatory response that leads to an increase in other cytokine levels that have similar effects (Chaudhry et al., 2011; Hoeppli et al., 2015). Thus, one would expect a difference between control and knockout animals only for certain cytokines, when no molecular compensation from other immune pathways are missing. In this sense, it is possible that the lack of differences between wild C57 and IL-10 knockout animals may be due to a molecular compensation mechanism still poorly understood. Studies using IL-10 knockout mice observed a chronic inflammatory response by gut-associated bacteria (Grunau et al., 2017; Lennon et al., 2018). It is now well described that success in wound repair requires a balance in the production of pro and anti-inflammatory mediators, since an excessive or prolonged inflammatory response can lead to tissue injury (Eming et al., 2007). Therefore, we believe that *C. urucurana* ointment may have positively affected the inflammatory response. Phenolic compounds present in *C. urucurana,* such as proanthocyanidins, create a protective layer on the surface of the wound and this physical barrier protects the infection lesion region, preventing the chronification of inflammation (Namjoyan et al., 2016). On the other hand, the flavonoid-enriched extract also regulates *in vivo* cellular activities related not only to fibroblasts (Nazaruk and Galicka, 2014) but also to mast cells, macrophages and lymphocytes (Lima et al., 2014; Meijer et al., 2015).

Despite the increased IL-2 and INF on day 7, when the inflammatory process reached its peak, we can suggest that the CR1 and CR2 was effective in modulating the inflammatory response, since, on the 14th day, all pro-inflammatory cytocines remained low, except for the 1% silver sulfadiazine group. These findings suggest that the inflammatory

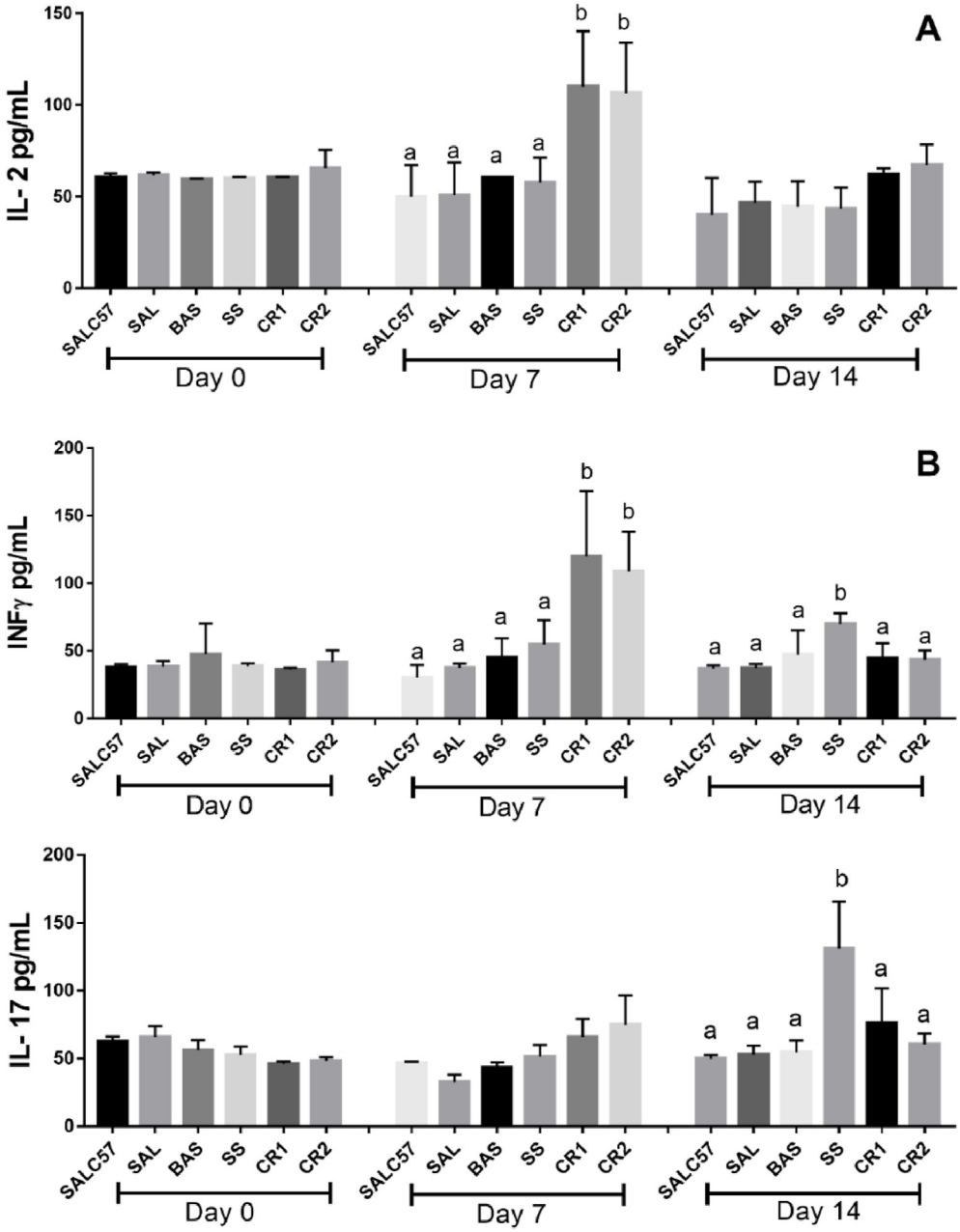

Fig. 6. Levels of proinflammatory cytokines: A-Interleukin-2 (IL-2), B-Interferon gamma (INF-gamma) and C-Interleukin-17 (IL-17) in the scar tissue of wild C57 mice and mice IL-10 knockout on days 0, 7, and 14. SalC57: C57 wild group, 0.9% saline solution. IL-10 knockout groups: SAL, 0.9% saline; BAS, Ointment Base; SS, 1% silver sulfadiazine; CR1, ointment of *C. urucurana* 5%; CR2, ointment of *C. urucurana* 10%. Data are represented as mean ± SD. Different letters indicate significant differences between groups $p < 0.05$ (Kruskal-Wallis test).

process was prolonged in the SS-treated group and may explain the delayed wound closure. This result showed that the SS group was similar to the control groups, which received no treatment.

In the present study, it was observed a high level of IL-4, a cytokine involved in the activation of mast cells and the resolution of inflammation (Serezani et al., 2017), in the groups CR1 and CR2. These findings are possibly related to the high anti-inflammatory power exerted by the *C. urucurana* extract. Studies have reported that the extract enriched by flavonoids, tannins, and alkaloids found in some plant species may have high immunostimulatory activity involved in the strengthening of the immune system (Khodadadi, 2015; Pérez-Cano and Castell, 2016). Cordeiro et al. (2016) also showed that the methanolic extract of *C. urucurana* peels tested at different doses may reduce the nociceptive effect caused by cytokines. Furthermore, herbal medicines and natural products may play an important role in the stimulation of cell proliferation, induction of collagen synthesis and improvement of the innate immune response of the wound (Bueno et al., 2014; Coelho et al., 2016; Gonçalves et al., 2016).

4. Conclusion

Our results indicate that the ointment developed from the *C. urucurana* bark extract has the potential to accelerate the closure of cutaneous wounds in 7 and 14 days and that *C. urucurana* is more effective at forming a strong scar when compared to silver sulfadiazine. This extract promotes qualitative and quantitative benefits to the cicatricial process by the modulation of the morphology in the damaged tissue and control of the inflammatory process, besides stimulating the cutaneous

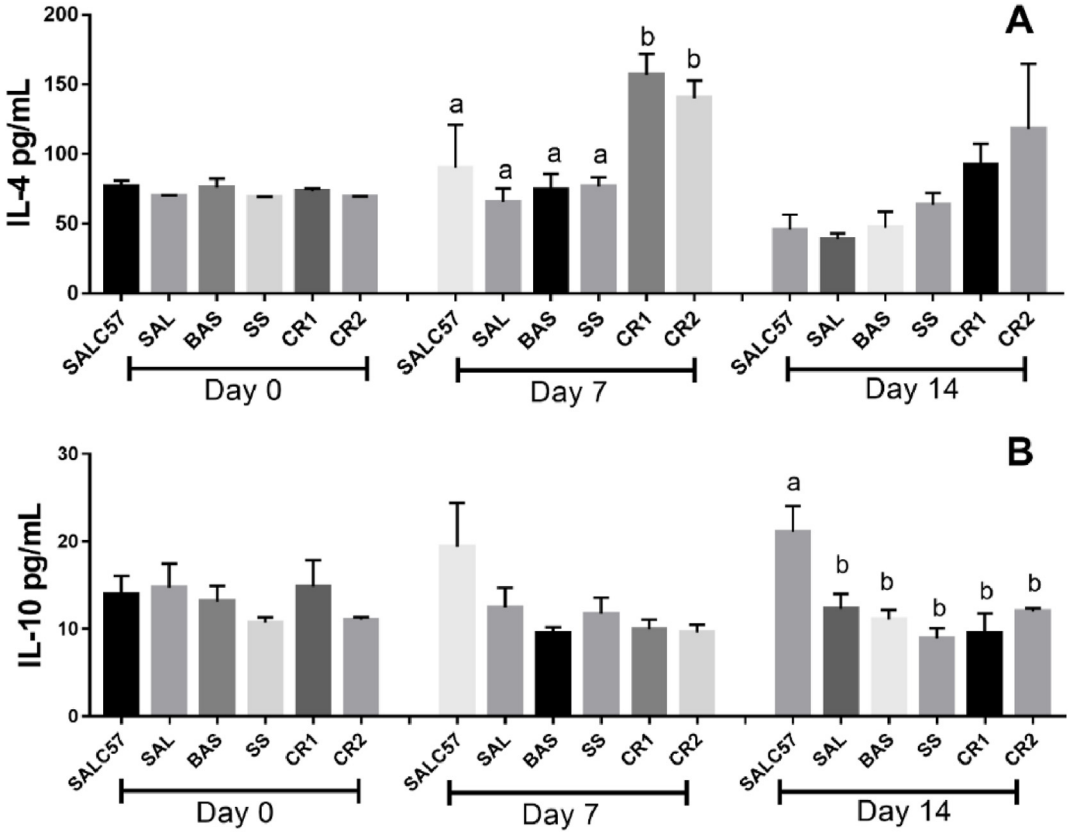

Fig. 7. Levels of anti-inflammatory cytokines: A-Interleukin-4 (IL-4), B-Interleukin-10 (IL-10) in the cicatricial tissue of wild C57 mice and IL-10 knockout mice on days 0, 7, and 14. SALC57: wild type C57 group, 0.9% saline solution. IL-10 knockout groups: SAL, 0.9% saline; BAS, Ointment Base; SS, 1% silver sulfadiazine; CR1, ointment of *C. urucurana* 5%; CR2, ointment of *C. urucurana* 10%. Data are represented as mean ± SD. Different letters indicate significant differences between groups $p < 0.05$ (Kruskal-Wallis test).

antioxidant defense systems. These effects can be attributed to the high content of phenolic compounds in the extract.

Author contributions

Formal analysis: Thalia del Rosario Loyo Casao, Camila Graça Pinheiro, Mariáurea Matias Sarandy, Ana Caroline Zanatta, Wagne Vilegas, Rômulo Dias Novaes.

Writing: Thalia del Rosario Loyo Casao, Camila Graça Pinheiro, Mariáurea Matias Sarandy.

Review and writing: João Paulo Viana, Reggiani Vilela Gonçalves.

Project administration and supervision: João Paulo Viana, Reggiani Vilela Gonçalves.

Funding

The authors are grateful to the support provided by Fundação do Amparo à Pesquisa do Estado de Minas Gerais (FAPEMIG, processes APQ-01895-16, PPM-00687-17 and PPM-00077-18), Conselho Nacional de Desenvolvimento Científico e Tecnológico (CNPq, processes 303972/2017–3, 423594/2018–4, 305093/2017–7 and MCTIC 408503/2018–1), and Coordenação de Aperfeiçoamento de Pessoal de Nível Superior -Brazil (CAPES, finance code 001).

Declaration of competing interest

None.

Acknowledgments

We are grateful to the Fundação de Amparo à Pesquisa do Estado de Minas Gerais (FAPEMIG).

Appendix A. Supplementary data

Supplementary data to this article can be found online at https://doi.org/10.1016/j.jep.2020.113042.

References

Abdulkhaleq, L.A., Assi, M.A., Abdullah, R., Zamri-Saad, M., Taufiq-Yap, Y.H., Hezmee, M.N.M., 2018. The crucial roles of inflammatory mediators in inflammation: a review. Vet. World 11, 627–635. https://doi.org/10.14202/vetworld.2018.627-635.

Afendi, F.M., Okada, T., Yamazaki, M., Hirai-Morita, A., Nakamura, Y., Nakamura, K., Ikeda, S., Takahashi, H., Altaf-Ul-Amin, M., Darusman, L.K., Saito, K., Kanaya, S., 2012. KNApSAcK family databases: integrated metabolite–plant species databases for multifaceted plant research. Plant Cell Physiol. 53https://doi.org/10.1093/pcp/pcr165. e1–e1.

Amorim, J.L., Figueiredo, J. de B., Amaral, A.C.F., Barros, E.G. de O., Palmero, C., MPalantinos, M.A., Ramos, A. de S., Ferreira, J.L.P., Silva, J.R. de A., Benjamim, C.F., Basso, S.L., Nasciutti, L.E., Fernandes, P.D., 2017. Wound healing properties of Copaifera paupera in diabetic mice. PloS One 12, e0187380. https://doi.org/10.1371/journal.pone.0187380.

Antunes-Neto, J.M.F., Silva, L.P., Macedo, D.V., 2006. Biomarcadores de estresse oxidativo: novas possibilidades de monitoramento. Rev. Bras. Ciência Mov. 13, 73–79. https://doi.org/10.18511/rbcm.v13i3.648.

Beecher, G.R., 2004. Proanthocyanidins: biological activities associated with human Health. Pharm. Biol. 42, 2–20. https://doi.org/10.3109/13880200490893474.

Bueno, F.G., Panizzon, G.P., Mello, E.V.S. de L., Lechtenberg, M., Petereit, F., Mello, J.C.P. de, Hensel, A., 2014. Hydrolyzable tannins from hydroalcoholic extract from Poincianella pluviosa stem bark and its wound-healing properties: phytochemical investigations and influence on in vitro cell physiology of human keratinocytes and dermal fibroblasts. Fitoterapia 99, 252–260. https://doi.org/10.1016/j.fitote.2014.10.007.

Chaudhry, A., Samstein, R.M., Treuting, P., Liang, Y., Pils, M.C., Heinrich, J.-M., Jack, R.S., Wunderlich, F.T., Brüning, J.C., Müller, W., Rudensky, A.Y., 2011. Interleukin-10 signaling in regulatory T cells is required for suppression of Th17 cell-mediated inflammation. Immunity 34, 566–578. https://doi.org/10.1016/j.immuni.2011.03.018.

Coelho, G.D.P., Martins, V.S., Amaral, L.V. do, Novaes, R.D., Sarandy, M.M., Gonçalves, R.V., 2016. Applicability of isolates and fractions of plant extracts in murine models in type II diabetes: a systematic review. Evidence-based complement. Alternative Med. 1–25https://doi.org/10.1155/2016/3537163. 2016.

Cordeiro, K.W., Felipe, J.L., Malange, K.F., do Prado, P.R., de Oliveira Figueiredo, P., Garcez, F.R., de Cássia Freitas, K., Garcez, W.S., Toffoli-Kadri, M.C., 2016. Anti-inflammatory and antinociceptive activities of Croton urucurana Baillon bark. J. Ethnopharmacol. 183, 128–135. https://doi.org/10.1016/j.jep.2016.02.051.

Eming, S.A., Krieg, T., Davidson, J.M., 2007. Inflammation in wound repair: molecular and cellular mechanisms. J. Invest. Dermatol. 127, 514–525. https://doi.org/10.1038/sj.jid.5700701.

Farahpour, M.R., Mirzakhani, N., Doostmohammadi, J., Ebrahimzadeh, M., 2015. Hydroethanolic Pistacia atlantica hulls extract improved wound healing process; evidence for mast cells infiltration, angiogenesis and RNA stability. Int. J. Surg. 17, 88–98. https://doi.org/10.1016/j.ijsu.2015.03.019.

Ferreira, F.V., Paula, L.B. De, 2013. Sulfadiazina de prata versus medicamentos fitoterápicos: estudo comparativo dos efeitos no tratamento de queimaduras Silver sulfadiazine versus herbal medicines : a comparative study of the effects in the treatment of burn injuries. Rev. Bras. Queimaduras 12, 132–139.

Fisher, N.M., Marsh, E., Lazova, R., 2003. Scar-localized argyria secondary to silver sulfadiazine cream. J. Am. Acad. Dermatol. 49, 730–732. https://doi.org/10.1067/S0190-9622(02)61574-9.

Fronza, M., Caetano, G.F., Leite, M.N., Bitencourt, C.S., Paula-Silva, F.W.G., Andrade, T.A.M., Frade, M.A.C., Merfort, I., Faccioli, L.H., 2014. Hyaluronidase modulates inflammatory response and accelerates the cutaneous wound healing. PloS One 9, e112297. https://doi.org/10.1371/journal.pone.0112297.

Fujiwara, T., Duscher, D., Rustad, K.C., Kosaraju, R., Rodrigues, M., Whittam, A.J., Januszyk, M., Maan, Z.N., Gurtner, G.C., 2016. Extracellular superoxide dismutase deficiency impairs wound healing in advanced age by reducing neovascularization and fibroblast function. Exp. Dermatol. 25, 206–211. https://doi.org/10.1111/exd.12909.

Ganeshkumar, M., Ponrasu, T., Krithika, R., Iyappan, K., Gayathri, V.S., Suguna, L., 2012. Topical application of Acalypha indica accelerates rat cutaneous wound healing by up-regulating the expression of Type I and III collagen. J. Ethnopharmacol. 142, 14–22. https://doi.org/10.1016/j.jep.2012.04.005.

Gonçalves, R.V., Novaes, R.D., Sarandy, M.M., Damasceno, E.M., Da Matta, S.L.P., De Gouveia, N.M., Freitas, M.B., Espindola, F.S., 2016. 5α-Dihydrotestosterone enhances wound healing in diabetic rats. Life Sci. 152, 67–75. https://doi.org/10.1016/j.lfs.2016.03.019.

Gonçalves, R.V., Novaes, R.D., Sarandy, M.M., Leite, J.P.V., Vilela, E.F., Cupertino, M. do C., da Matta, S.L.P., 2016. Schizocalyx cuspidatus (A. St.-Hil.) Kainul. & B. Bremer extract improves antioxidant defenses and accelerates the regression of hepatic fibrosis after exposure to carbon tetrachloride in rats. Nat. Prod. Res. 30, 2738–2742. https://doi.org/10.1080/14786419.2016.1143825.

Gonzalez, A.C. de O., Costa, T.F., Andrade, Z. de A., Medrado, A.R.A.P., 2016. Wound healing - a literature review. An. Bras. Dermatol. 91, 614–620. https://doi.org/10.1590/abd1806-4841.20164741.

Grunau, A., Escher, U., Bereswill, S., Heimesaat, M.M., 2017. Toll-like receptor-4 dependent inflammatory responses following intestinal colonization of secondary abiotic IL10-deficient mice with multidrug-resistant Pseudomonas aeruginosa. Eur. J. Microbiol. Immunol. 7, 210–219. https://doi.org/10.1556/1886.2017.00023.

Guo, S., DiPietro, L.A., 2010. Factors affecting wound healing. J. Dent. Res. 89, 219–229. https://doi.org/10.1177/0022034509359125.

Gupta, D., Bleakley, B., Gupta, R.K., 2008. Dragon's blood: botany, chemistry and therapeutic uses. J. Ethnopharmacol. 115, 361–380. https://doi.org/10.1016/j.jep.2007.10.018.

Habig, W.H., Pabst, M.J., Jakoby, W.B., 1976. Glutathione S-transferase AA from rat liver. Arch. Biochem. Biophys. 175, 710–716. https://doi.org/10.1016/0003-9861(76)90563-4.

Hemmati, A.A., Foroozan, M., Houshmand, G., Moosavi, Z.B., Bahadoram, M., Maram, N.S., 2014. The topical effect of grape seed extract 2% cream on surgery wound healing. Global J. Health Sci. 7, 52–58. https://doi.org/10.5539/gjhs.v7n3p52.

Hoeppli, R.E., Wu, D., Cook, L., Levings, M.K., 2015. The environment of regulatory T cell biology: cytokines, metabolites, and the microbiome. Front. Immunol. 6. https://doi.org/10.3389/fimmu.2015.00061.

Horai, H., Arita, M., Kanaya, S., Nihei, Y., Ikeda, T., Suwa, K., Ojima, Y., Tanaka, Kenichi, Tanaka, S., Aoshima, K., Oda, Y., Kakazu, Y., Kusano, M., Tohge, T., Matsuda, F., Sawada, Y., Hirai, M.Y., Nakanishi, H., Ikeda, K., Akimoto, N., Maoka, T., Takahashi, H., Ara, T., Sakurai, N., Suzuki, H., Shibata, D., Neumann, S., Iida, T., Tanaka, Ken, Funatsu, K., Matsuura, F., Soga, T., Taguchi, R., Saito, K., Nishioka, T., 2010. MassBank: a public repository for sharing mass spectral data for life sciences. J. Mass Spectrom. 45, 703–714. https://doi.org/10.1002/jms.1777.

Hou, M., Man, M., Man, W., Zhu, W., Hupe, M., Park, K., Crumrine, D., Elias, P.M., Man, M.-Q., 2012. Topical hesperidin improves epidermal permeability barrier function and epidermal differentiation in normal murine skin. Exp. Dermatol. 21, 337–340. https://doi.org/10.1111/j.1600-0625.2012.01455.x.

Hou, M., Sun, R., Hupe, M., Kim, P.L., Park, K., Crumrine, D., Lin, T.-K., Santiago, J.L., Mauro, T.M., Elias, P.M., Man, M.-Q., 2013. Topical apigenin improves epidermal permeability barrier homoeostasis in normal murine skin by divergent mechanisms. Exp. Dermatol. 22, 210–215. https://doi.org/10.1111/exd.12102.

Hsu, P., Santner-Nanan, B., Hu, M., Skarratt, K., Lee, C.H., Stormon, M., Wong, M., Fuller, S.J., Nanan, R., 2015. IL-10 potentiates differentiation of human induced regulatory T cells via STAT3 and Foxo 1. J. Immunol. 195, 3665–3674. https://doi.org/10.4049/jimmunol.1402898.

Jara, C.P., Bóbbo, V.C.D., Carraro, R.S., de Araujo, T.M.F., Lima, M.H.M., Velloso, L.A., Araújo, E.P., 2018. Effects of topical topiramate in wound healing in mice. Arch. Dermatol. Res. 310, 363–373. https://doi.org/10.1007/s00403-018-1822-z.

Johnson, K.E., Wilgus, T.A., 2014. Vascular endothelial growth factor and angiogenesis in the regulation of cutaneous wound repair. Adv. Wound Care 3, 647–661. https://doi.org/10.1089/wound.2013.0517.

Kant, V., Gopal, A., Kumar, Dhirendra, Pathak, N.N., Ram, M., Jangir, B.L., Tandan, S.K., Kumar, Dinesh, 2015. Curcumin-induced angiogenesis hastens wound healing in diabetic rats. J. Surg. Res. 193, 978–988. https://doi.org/10.1016/j.jss.2014.10.019.

Khezri, K., Farahpour, M.R., Mounesi Rad, S., 2019. Accelerated infected wound healing by topical application of encapsulated Rosemary essential oil into nanostructured lipid carriers. Artif. Cells, Nanomedicine, Biotechnol. 47, 980–988. https://doi.org/10.1080/21691401.2019.1582539.

Khodadadi, S., 2015. Role of herbal medicine in boosting immune system. Immunopathol. Persa 1, 4–5.

Krystel-Whittemore, M., Dileepan, K.N., Wood, J.G., 2016. Mast Cell: a multi-functional master cell. Front. Immunol. 6, 1–12. https://doi.org/10.3389/fimmu.2015.00620.

Landén, N.X., Li, D., Ståhle, M., 2016. Transition from inflammation to proliferation: a critical step during wound healing. Cell. Mol. Life Sci. 73, 3861–3885. https://doi.org/10.1007/s00018-016-2268-0.

Leclere, M., Desnoyers, M., Beauchamp, G., Lavoie, J., 2006. Comparison of four staining methods for detection of mast cells in equine bronchoalveolar lavage fluid. J. Vet. Intern. Med. 20, 377–381. https://doi.org/10.1111/j.1939-1676.2006.tb02871.x.

Lennon, E.M., Borst, L.B., Edwards, L.L., Moeser, A.J., 2018. Mast Cells exert anti-inflammatory effects in an IL10 −/− model of spontaneous colitis. Mediat. Inflamm. 1–13. https://doi.org/10.1155/2018/7817360. 2018.

Lima, L.D., Andrade, S.P., Campos, P.P., Barcelos, L.S., Soriani, F.M., AL Moura, S., Ferreira, M.A., 2014. Brazilian green propolis modulates inflammation, angiogenesis and fibrogenesis in intraperitoneal implant in mice. BMC Compl. Alternative Med. 14, 177. https://doi.org/10.1186/1472-6882-14-177.

Limón-Pacheco, J., Gonsebatt, M.E., 2009. The role of antioxidants and antioxidant-related enzymes in protective responses to environmentally induced oxidative stress. Mutat. Res. Toxicol. Environ. Mutagen. 674, 137–147. https://doi.org/10.1016/j.mrgentox.2008.09.015.

Lopes, T.V., Félix, S.R., Schons, S. de V., Nobre, M. de O., 2013. Dragon's blood (Croton lechleri Mull., Arg.): an update on the chemical composition and medical applications of this natural plant extract. A review. Rev. Bras. Hig. e Sanidade Anim. 7, 167–191. https://doi.org/10.5935/1981-2965.20130016.

Lowry, O.H., Rosebrough, N.J., Farr, A.L., Randall, R.J., 1951. Protein measurement with the folin phenol reagent. J. Biol. Chem. 193, 265–275.

Machado, L.C.D.S., Araci, I., Pfrimer, H., Magalhães, M.R., 2015. Cicatrização de feridas induzidas por peçonha de Bothrops Moojeni pelo extrato de Croton urucurana. Estudos 42, 597–611.

Man, M., Hupe, M., Mackenzie, D., Kim, H., Oda, Y., Crumrine, D., Lee, S.H., Martin-Ezquerra, G., Trullas, C., Mauro, T.M., Feingold, K.R., Elias, P.M., Man, M.-Q., 2011. A topical Chinese herbal mixture improves epidermal permeability barrier function in normal murine skin. Exp. Dermatol. 20, 285–288. https://doi.org/10.1111/j.1600-0625.2010.01205.x.

Manzuoerh, R., Farahpour, M.R., Oryan, A., Sonboli, A., 2019. Effectiveness of topical administration of Anethum graveolens essential oil on MRSA-infected wounds. Biomed. Pharmacother. 109, 1650–1658. https://doi.org/10.1016/j.biopha.2018.10.117.

Meijer, K., Vonk, R.J., Priebe, M.G., Roelofsen, H., 2015. Cell-based screening assay for anti-inflammatory activity of bioactive compounds. Food Chem. 166, 158–164. https://doi.org/10.1016/j.foodchem.2014.06.053.

Modarresi, M., Farahpour, M.-R., Baradaran, B., 2019. Topical application of Mentha piperita essential oil accelerates wound healing in infected mice model. Inflammopharmacology 27, 531–537. https://doi.org/10.1007/s10787-018-0510-0.

Morry, J., Ngamcherdtrakul, W., Yantasee, W., 2017. Oxidative stress in cancer and fibrosis: opportunity for therapeutic intervention with antioxidant compounds, enzymes, and nanoparticles. Redox Biol 11, 240–253. https://doi.org/10.1016/j.redox.2016.12.011.

Muthusubramaniam, L., Zaitseva, T., Paukshto, M., Martin, G., Desai, T., 2014. Effect of collagen nanotopography on keloid fibroblast proliferation and matrix synthesis: implications for dermal wound healing. Tissue Eng. 20, 2728–2736. https://doi.org/10.1089/ten.tea.2013.0539.

Namjoyan, F., Kiashi, F., Moosavi, Z.B., Saffari, F., Makhmalzadeh, B.S., 2016. Efficacy of Dragon's blood cream on wound healing: a randomized, double-blind, placebo-controlled clinical trial. J. Tradit. Complement. Med. 6, 37–40. https://doi.org/10.1016/j.jtcme.2014.11.029.

Nazaruk, J., Galicka, A., 2014. The influence of selected flavonoids from the leaves of Cirsium palustre (L.) Scop. on collagen expression in human skin fibroblasts. Phyther. Res. 28, 1399–1405. https://doi.org/10.1002/ptr.5143.

Novaes, R.D., Cupertino, M.C., Sarandy, M.M., Souza, A., Soares, E.A., Gonçalves, R.V., 2015. Time-Dependent resolution of collagen deposition during skin repair in rats: a correlative morphological and biochemical study. Microsc. Microanal. 21, 1482–1490. https://doi.org/10.1017/S1431927615015366.

Oliveira, C.M.B. de, Sakata, R.K., Issy, A.M., Gerola, L.R., Salomão, R., 2011. Citocinas e dor. Rev. Bras. Anestesiol. 61, 260–265. https://doi.org/10.1590/S0034-70942011000200014.

Patil, M.V.K., Kandhare, A.D., Bhise, S.D., 2012. Pharmacological evaluation of ethanolic extract of Daucus carota Linn root formulated cream on wound healing using excision and incision wound model. Asian Pacific J. Trop. Biomed. S646–S655 2012.

Pérez-Cano, F., Castell, M., 2016. Flavonoids, inflammation and immune system. Nutrients 8, 659. https://doi.org/10.3390/nu8100659.
Ragonha, A.C.O., Ferreira, E., Andrade, D. de, Rossi, L.A., 2005. Avaliação microbiológica de coberturas com sulfadiazina de prata a 1%, utilizadas em queimaduras. Rev. Lat. Am. Enfermagem 13, 514–521. https://doi.org/10.1590/S0104-11692005000400009.
Rieder, A., Figueiredo, G., Pereira, E., 2011. Plant known as „Sangra d'água" (Croton urucurana Baill. (Euphorbiaceae) and its medicinal use in southwestern of Mato Grosso state, Brazil. Planta Med. 77, 1327. https://doi.org/10.1055/s-0031-1282473.
Roleira, F.M.F., Tavares-da-Silva, E.J., Varela, C.L., Costa, S.C., Silva, T., Garrido, J., Borges, F., 2015. Plant derived and dietary phenolic antioxidants: anticancer properties. Food Chem. 183, 235–258. https://doi.org/10.1016/j.foodchem.2015.03.039.
Rosa, D.F., Sarandy, M.M., Novaes, R.D., Freitas, M.B., do Carmo Gouveia Pelúzio, M., Gonçalves, R.V., 2018. High-fat diet and alcohol intake promotes inflammation and impairs skin wound healing in wistar rats. Mediat. Inflamm. 1–12. https://doi.org/10.1155/2018/4658583. 2018.
Salatino, A., Salatino, M.L.F., Negri, G., 2007. Traditional uses, chemistry and pharmacology of Croton species (Euphorbiaceae). J. Braz. Chem. Soc. 18, 11–33. https://doi.org/10.1590/S0103-50532007000100002.
Salinas-Sánchez, D., Jiménez-Ferrer, E., Sánchez-Sánchez, V., Zamilpa, A., González-Cortazar, M., Tortoriello, J., Herrera-Ruiz, M., 2017. Anti-inflammatory activity of a polymeric proanthocyanidin from serjania schiedeana. Molecules 22, 863. https://doi.org/10.3390/molecules22060863.
Salvi, M., Battaglia, V., Brunati, A.M., La Rocca, N., Tibaldi, E., Pietrangeli, P., Marcocci, L., Mondovì, B., Rossi, C.A., Toninello, A., 2007. Catalase takes part in rat liver mitochondria oxidative stress defense. J. Biol. Chem. 282, 24407–24415. https://doi.org/10.1074/jbc.M701589200.
Samy, R.P., Kandasamy, M., Gopalakrishnakone, P., Stiles, B.G., Rowan, E.G., Becker, D., Shanmugam, M.K., Sethi, G., Chow, V.T.K., 2014. Wound healing activity and mechanisms of action of an antibacterial protein from the venom of the eastern diamondback rattlesnake (Crotalus adamanteus). PloS One 9, e80199. https://doi.org/10.1371/journal.pone.0080199.
Sarandy, M.M., Miranda, L.L., Altoé, L.S., Novaes, R.D., Zanuncio, V.V., Leite, J.P.V., Gonçalves, R.V., 2018. Strychnos pseudoquina modulates the morphological reorganization of the scar tissue of second intention cutaneous wounds in rats. PloS One 13, e0195786. https://doi.org/10.1371/journal.pone.0195786.
Sarandy, M.M., Novaes, R.D., da Matta, S.L.P., Mezencio, J.M. da S., da Silva, M.B., Zanuncio, J.C., Gonçalves, R.V., 2015. Ointment of Brassica oleracea var. capitata matures the extracellular matrix in skin wounds of wistar rats. Evidence-based complement. Alternative Med. 1–9https://doi.org/10.1155/2015/919342. 2015.
Sarandy, M.M., Novaes, R.D., Xavier, A.A., Vital, C.E., Leite, J.P.V., Melo, F.C.S.A., Gonçalves, R.V., 2017. Hydroethanolic extract of *Strychnos pseudoquina* accelerates skin wound healing by modulating the oxidative status and microstructural reorganization of scar tissue in experimental type I diabetes. BioMed Res. Int. 1–11. https://doi.org/10.1155/2017/9538351. 2017.
Schmidt, C.A., Murillo, R., Heinzmann, B., Laufer, S., Wray, V., Merfort, I., 2011. Structural and conformational analysis of proanthocyanidins from Parapiptadenia rigida and their wound-healing properties. J. Nat. Prod. 74, 1427–1436. https://doi.org/10.1021/np200158g.
Serezani, A.P., Bozdogan, G., Sehra, S., Walsh, D., Krishnamurthy, P., Sierra Potchanant, E.A., Nalepa, G., Goenka, S., Turner, M.J., Spandau, D.F., Kaplan, M.H., 2017. IL-4 impairs wound healing potential in the skin by repressing fibronectin expression. J. Allergy Clin. Immunol. 139, 142–151. https://doi.org/10.1016/j.jaci.2016.07.012. e5.
Shapira, S., Ben-Amotz, O., Sher, O., Kazanov, D., Mashiah, J., Kraus, S., Gur, E., Arber, N., 2015. Delayed wound healing in heat stable antigen (HSA/CD24)-deficient mice. PloS One 10, e0139787. https://doi.org/10.1371/journal.pone.0139787.
Shedoeva, A., Leavesley, D., Upton, Z., Fan, C., 2019. Wound healing and the use of medicinal plants. Evidence-based complement. Alternative Med. 1–30. https://doi.org/10.1155/2019/2684108. 2019.
Siddiqui, I.A., Raisuddin, S., Shukla, Y., 2005. Protective effects of black tea extract on testosterone induced oxidative damage in prostate. Canc. Lett. 227, 125–132. https://doi.org/10.1016/j.canlet.2004.10.046.
Silva, F.M.A. da, Koolen, H.H.F., Almeida, R.A. de, Souza, A.D.L. de, Pinheiro, M.L.B., Costa, E.V., 2012. Desreplicação de alcaloides aporfínicos e oxoaporfínicos de Unonopsis guatterioides por ESI-IT-MS. Quim. Nova 35, 944–947. https://doi.org/10.1590/S0100-40422012000500015.
Smith, C.A., Maille, G.O., Want, E.J., Qin, C., Trauger, S.A., Brandon, T.R., Custodio, D.E., Abagyan, R., Siuzdak, G., 2005. METLIN. Ther. Drug Monit. 27, 747–751. https://doi.org/10.1097/01.ftd.0000179845.53213.39.
Tala, V., Candida da Silva, V., Rodrigues, C., Nkengfack, A., Campaner dos Santos, L., Vilegas, W., 2013. Characterization of proanthocyanidins from parkia biglobosa (Jacq.) G. Don. (Fabaceae) by flow injection analysis — electrospray ionization ion trap tandem mass spectrometry and liquid chromatography/electrospray ionization mass spectrometry. Molecules 18, 2803–2820. https://doi.org/10.3390/molecules18032803.
Tang, J., Liu, H., Gao, C., Mu, L., Yang, S., Rong, M., Zhang, Z., Liu, J., Ding, Q., Lai, R., 2014. A Small peptide with potential ability to promote wound healing. PloS One 9, e92082. https://doi.org/10.1371/journal.pone.0092082.
Tatsuno, T., Jinno, M., Arima, Y., Kawabata, T., Hasegawa, T., Yahagi, N., Takano, F., Ohta, T., 2012. Anti-inflammatory and anti-melanogenic proanthocyanidin oligomers from peanut skin. Biol. Pharm. Bull. 35, 909–916. https://doi.org/10.1248/bpb.35.909.
Thakur, R., Jain, N., Pathak, R., Sandhu, S.S., 2011. Practices in wound healing studies of plants. Evidence-Based Complement. Alternative Med. 1–17. https://doi.org/10.1155/2011/438056. 2011.
Thandavarayan, R.A., Garikipati, V.N.S., Joladarashi, D., Suresh Babu, S., Jeyabal, P., Verma, S.K., Mackie, A.R., Khan, M., Arumugam, S., Watanabe, K., Kishore, R., Krishnamurthy, P., 2015. Sirtuin-6 deficiency exacerbates diabetes-induced impairment of wound healing. Exp. Dermatol. 24, 773–778. https://doi.org/10.1111/exd.12762.
Tsuchiya, H., 2015. Membrane interactions of phytochemicals as their molecular mechanism applicable to the discovery of drug leads from plants. Molecules 20, 18923–18966. https://doi.org/10.3390/molecules201018923.
Valero, C., Javierre, E., García-Aznar, J.M., Gómez-Benito, M.J., 2014. A Cell-Regulatory mechanism involving feedback between contraction and tissue formation guides wound healing progression. PloS One 9, e92774. https://doi.org/10.1371/journal.pone.0092774.
Venkatesha, S.H., Berman, B.M., Moudgil, K.D., 2011. Herbal medicinal products target defined biochemical and molecular mediators of inflammatory autoimmune arthritis. Bioorg. Med. Chem. 19, 21–29. https://doi.org/10.1016/j.bmc.2010.10.053.
Wen-Guang, L., Xiāo-Yu, Z., Yong-Jie, W., Xuan, T., 2001. Anti-inflammatory effect and mechanism of proanthocyanidins from grape seeds. Acta Pharmacol. Sin. 12, 1117–1120.
Wolff, K.C., Pinto, L.A., Formagio, A.S.N., Faloni de Andrade, S., Kassuya, C.A.L., Freitas, K. de C., 2012. Antiulcerogenic effect of Croton urucurana Baillon bark. J. Ethnopharmacol. 143, 331–337. https://doi.org/10.1016/j.jep.2012.06.044.
Yan, R., Wang, W., Guo, J., Liu, H., Zhang, J., Yang, B., 2013. Studies on the alkaloids of the bark of Magnolia officinalis: isolation and on-line analysis by HPLC-ESI-MSn. Molecules 18, 7739–7750. https://doi.org/10.3390/molecules18077739.